ISSN: 1999-1630

SEU Journal of Science and Engineering, Vol. 13, No. 1, June 2019

Design and Simulation of a DC microgrid for a remote Island (Sandwip)

Sk. Md. Golam Mostafa[1], Al Shahriar Pial[2], Md Jonayed Hossen[3*], Md. Sultan Mahmud[4], Md. Ashabus Sayeed Chowdhury[5]

[12345]*Department of Electrical and Electronic Engineering, International Islamic University Chittagong, Chittagong, Bangladesh*

Abstract

A microgrid based on direct current (DC) was designed and simulated for a small island in Sandwip. The energy generated in the microgrid will come from DC sources and the loads on the island will also be DC. Therefore, it was proposed to design a microgrid based on DC to reduce the number of conversion losses between AC-DC. A microgrid based on DC will have no power factor losses, fewer corona discharges due to the absence of the skin effect and allow for a cheaper and simpler system. DC microgrids are already widespread in the telecoms industry for data centers, airplanes, submarines, and remote locations. MATLAB/Simulink was used to design and simulate the individual components of the microgrid. The solar and wind resources for the island were modeled along with the predicted load profiles of the island. A financial analysis was conducted using the HOMER software. An AC microgrid with diesel only generation which is currently in use resulted in the highest overall costs, an AC-DC hybrid microgrid resulted in a cheaper system than the diesel-only system and a DC microgrid resulted in the lowest costs. Technical analysis of the DC microgrid was conducted. The microgrid would require 1.03% island cover from PV panels.

Keywords: DC Microgrid; DC Source; HOMER; MATLAB; Simulink

I. Introduction

Sandwip is located with coordinates 22.4919º N, 91.4209º E. Figure 1.1 shows its location on a map located offshore Kumira, Chittagong. According to a recent survey, the 762.42 square-kilometer off-shore island as a population of 4,72,179. Some 58,423 families are living under 15 unions and one municipality of the Upazila.

A direct current (DC) microgrid will be designed and simulated for a remote island (Sandwip). Most of the human beings of rural and some distant flung coastal regions use kerosene for lighting in addition to cooking alongside fireside woods. In some of the off-grid locations diesel generators, operated and maintained through personal marketers or cooperatives, are gambling the vital issue characteristic for supplying electricity for a few hours in the night time. Mostly those turbines are positioned inside the rural markets for meeting the lights call for of the stores and close by households. The fee of power from diesel generator end up in the variety from 15 to 32 Taka/kWh and typically the bill became gathered on each day foundation at a price of Taka three to eight consistent with lamp even as the price of diesel emerge as sixty-five Taka/liter. A DC microgrid will help to facilitate the integration of renewables and positively add to the image of the island.

Currently, in Sandwip, the authority supply 1MW of electricity to some parts of Sandwip from 6 pm to 12 am, through a diesel generator which allowed around 2000 people to use electricity [13]. If the total consumers of Sandwip are to be covered with diesel-based generator then there will be required huge capital and it is way more costly compared to our proposed microgrid design for Sandwip. Therefore, a DC microgrid is designed based on renewable energy which will be more feasible than diesel-based generator electricity generation.

*** Corresponding Author:** Md Jonayed Hossen, Department of Electrical and Electronic Engineering, International Islamic University Chittagong, Kumira, Chittagong, Bangladesh; Email: *jheee18.iiuc@gmail.com*

II. Theory

DC transmission is making a comeback and has the potential to provide many benefits especially with microgrids. Photovoltaic (PV) cells generate DC electricity and with the majority of electronic loads requiring DC, a DC microgrid would eliminate the conversion steps between AC and DC [9]. A traditional system would require the PV energy to be inverted from DC to AC so that the energy can be sent to the grid and then another conversion step inside the electronic load rectifying the electricity back from AC to DC so that the energy can be used. Therefore, because each conversion step introduces losses to the system, eliminating these two conversion steps has the potential to improve the efficiency of the DC microgrid by 10-25% [1]. Also, wind, small scale hydro and tidal power generation use variable-speed turbines which involve converting the variable AC energy from AC to DC and then back to AC at the required frequency as shown in Figure 2.1. Variable speed turbines are used to let the turbine rotate at a particular speed to extract maximum power from the resource. Due to the varying frequency, the energy is converted to DC and then the electricity can be converted back to AC at 50Hz. Therefore, the usage of a DC microgrid with these systems could nonetheless lessen a conversion step from DC to AC and enhance the performance of the system [6].

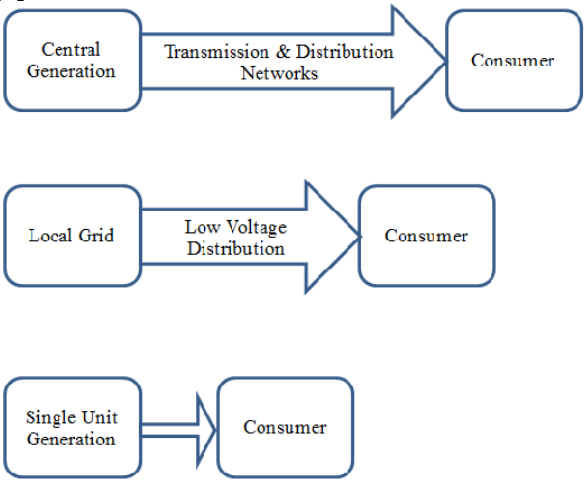

Figure 1: Three topologies of generation and evacuation of electricity in Bangladesh.

III. Methods

Simulink has an environment called Simscape which can be used to model dynamical systems with physical modelling by using equation-based representation and allows for bidirectional energy flows [3]. DC-DC converter, solar modules, wind turbines, batteries and a charge controller will be analysed.

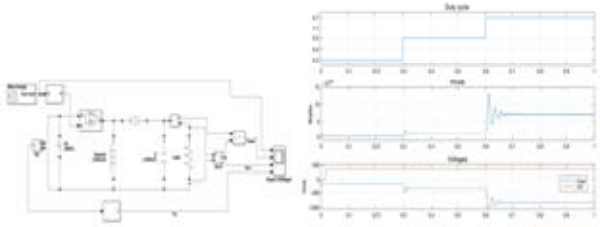

(a) Design in Simulink (b) Simulink output

Figure 2: Buck-Boost converter in Simulink.

The circuit of Figure 2(a) was simulated with a duty cycle of 0.3, 0.5 and 0.7. The simulation results can be seen in Figure 2(b). The buck-boost converter output in Figure 2(b) shows that when the duty cycle is equal to 0.5, the output voltage is equal to the input voltage. Also, when the duty cycle is above 0.5, the output voltage is greater than the input voltage and when the duty cycle is below 0.5, the output voltage is below the input voltage. When the duty cycle is 0.7, the output voltage was 840 V as can be confirmed using the following equation:

$$V_o = -V_s\left(\frac{D}{1-D}\right) = -360\left(\frac{0.7}{1-0.7}\right) = -840V$$

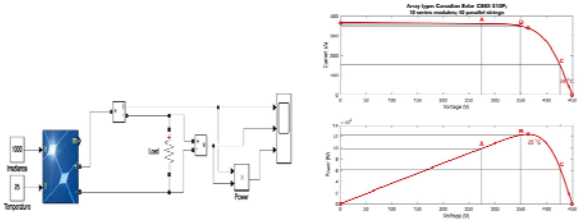

(a) PV circuit (b) PV output

Figure 3: PV array simulation in Simulink under standard test conditions.

The circuit of Figure 3(a) was simulated in Simulink under standard test conditions with an irradiance of 1000 W/m^2 and at 25°C. The PV curves under these conditions are shown in 3.15(b). The circuit was simulated with different

loads to investigate the power delivered by the PV array and to investigate the principle of maximum power transfer. Figure 3.16 shows the outputs from the simulations with the load at 0.75 Ω, 1 Ω and 3 Ω respectively. The results are summarized in Table 1.

When the load is at 0.75 Ω, the current, voltage and power are at 360.8 *A*, 270.6 *V,* and 97.6 *kW* respectively. On the curves of Figure 3(b) the PV array is operating at point A. When the load is at 1 Ω the current, voltage and power are at 349.7 *A*, 349.7 *V,* and 122.3 *kW* respectively. On the curves of Figure 3.15(b) the PV array is operating at point B. When the load is at 3 Ω the current, voltage and power are at 142.5 *A*, 427.4 *V,* and 60.88 *kW* respectively. On the curves of Figure 3(b) the PV array is operating at point C. As you can see, the power delivered by the PV array can be adjusted by varying the load resistance. Maximum power is transferred when the load resistance is equal to the resistance of the PV array.

Table 1: PV output vs change in load

Load (Ω)	Current (A)	Voltage (V)	Power (kW)
0.75	360.8	270.6	97.6
1	349.7	349.7	122.3
3	142.5	427.6	60.88

The power generated by a wind turbine is shown in the following Equation:

$$Pm = \frac{1}{2} \cdot \rho \cdot A \cdot C_p(\lambda, \beta) \cdot V_w^3$$

Where ρ is the air density, A is the rotor area that is swept, *Vw* is the wind speed and *Cp(γ,β)* is the power factor coefficient. *Cp(γ,β)* is a measure of the amount of energy extracted from the wind resource and is a function of a tip speed ratio *γ* and the pitch angle *β*. The Betz limits state that the power factor coefficient has a limit of 59.7%. The Tip speed ratio is the relative speed of the rotor and wind speed. The pitch angle is the relative angle between the rotor and the axis.

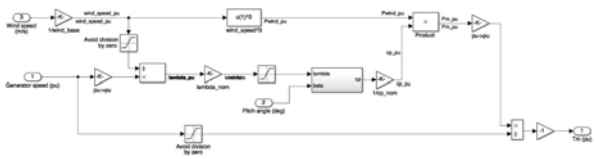

Figure 4: Simulink model of a wind turbine.

The power generated from a wind turbine is proportional to the cube of the wind speed. Therefore, wind turbines should be placed in areas of high mean annual wind speeds. If wind speeds are too high, pitch control can be applied where the angle of the blades is adjusted to reduce the speed of the blades. The Simulink diagram of a wind turbine is shown in Figure 4, which is based on wind speed Equation. Wind turbines start to produce power and wind speeds at around 3-4 m/s and are stopped in high wind speeds approximately above 20-25 m/s [8].

Simulink has a built-in component for a battery as shown in Figure 5(a). Figure 5(b) shows that when current is being delivered to the battery, the SOC increases and when current is being drawn from the battery, the SOC decreases. This built-in design will be used in conjunction with the designed DC microgrid.

(a)Battery circuit (b) Battery outputs

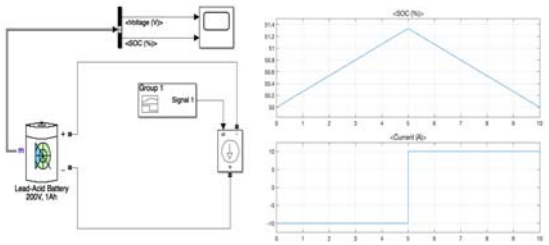

Figure 5: Simulink battery simulation.

Charge controllers are used to regulating the flow of current to and from batteries in a microgrid [11]. They are essential to protect the batteries and regulate the DC bus voltage. In this DC microgrid project, a charge controller will control a bidirectional converter lowering the PV output voltage produced to the level required by the batteries and when the PV output drops to zero, the charge controller will activate the bidirectional converter to send the power from the batteries to the microgrid. Figure 6 shows the proposed logic for a charge controller in a DC

microgrid. Most batteries are designed to operate in the region of 30-90%. Therefore, the logic in the controller will check if the batteries are in the region of 30-90% and if they are depending on the power balance between the generation and load, the batteries will either charge or discharge. If the batteries are at a low SOC of below 30% and if the power generated is greater than the required load, the batteries will be charged but if the load is higher than the power generated load shedding should be considered to protect the batteries. The last case is if the batteries are at a high SOC of above 90%. In this case, if the microgrid is generating excess power the current will be sent to a dump load to protect the batteries from overcharging and the DC bus voltage from increasing.

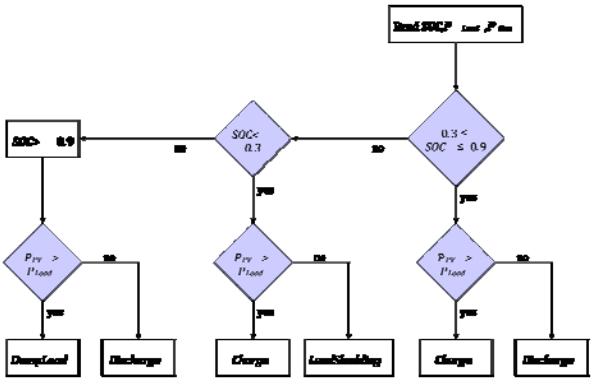

Figure 6: Charge controller logic.

The PI controller was implemented into Simulink using objects as shown in Figure 7. The proportional block was selected to be 0.02 and the integral block was selected as 3. The terms were added together and a limit was applied between 0.95 and -0.95 because the output will operate a bidirectional converter that has a maximum duty ratio of 1 but problems occur with infinity at 1 so 0.95 was chosen for the limits. The output is fed to the output y and the error is fed back into the input u. The output y will either be positive or negative depending on if the DC voltage needs to be increased or decreased. Therefore, logic will be used to transmit the positive signals to the boost control and the negative signals to the buck control of the bidirectional converter.

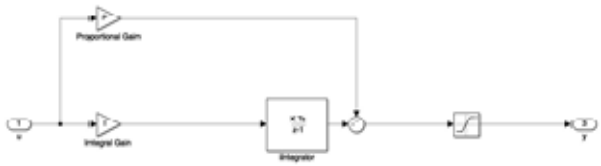

Figure 7: Simulink PI controller topology.

IV. Results

Firstly, the resources and components for the microgrid and list of their specifications will be described. Secondly, the results from the financial analysis which was conducted in order to select the most economical system that can meet the load requirements will be presented.

The solar data for Sandwip was loaded from the Hybrid Optimization Model for Electric Renewables (HOMER) [5] database by specifying the locations coordinates of 22.4919º N, 91.4209º E. Sandwip has a relatively strong solar resource with a daily radiation annual average of 4.51 $kWh/m^2/day$. A graph of the average daily radiation for each month is shown in Figure 8. The months from February to May have the greatest amounts of solar radiation but coexist with a greater amount of cloud cover indicated by the yellow line which is the clearness index. The average daily profile of solar radiation for each month is shown in Figure 9. As you can see the solar radiation starts to increase from 6am, peaking at around 12pm and returning to zero just after 6pm for all months but with variations in magnitude.

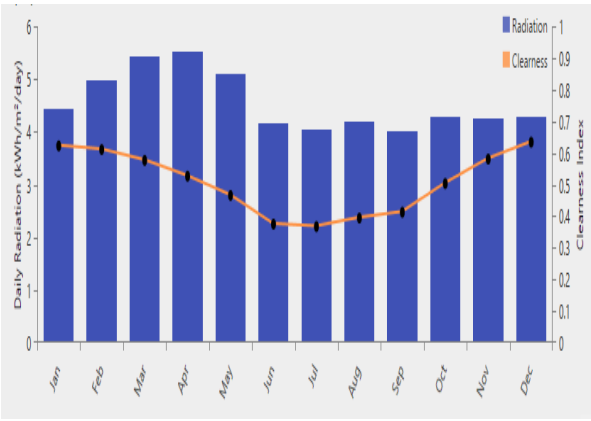

Figure 8: Average Daily Solar Radiation for each month at Sandwip.

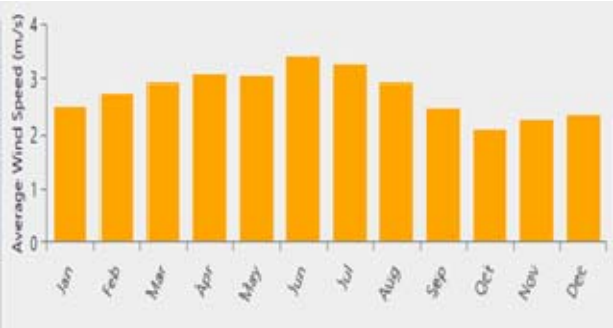

Figure 9: Average daily solar profile for each month at Sandwip.

The wind data for Sandwip was downloaded from the NREL database and was edited into the appropriate format to upload it into the HOMER software. The wind resource for Sandwip is not so strong with an annual average wind speed of 3.56 *m/s*. Figure 4.2(a) shows the average wind speeds for each month. Very low wind speeds can be seen in the months from October to December of below 3 *m/s*. As you can see the wind resource profile is much more random than the solar resource. The Weibull k distribution for the wind resource is 4.24. Weibull k factors indicate the data distribution with lower k values corresponding to broader distributions of wind speeds and higher k values corresponding to smaller wind speed distributions. The Weibull distribution of 4.24 is relatively high indicating that the region of Sandwip has a wide variance in wind speeds typical in gusty areas without a strong constant wind resource. Figure 4.2(b) shows the scaled data for each month. The strongest wind speeds are in June with maximum wind speeds exceeding 6 *m/s*.

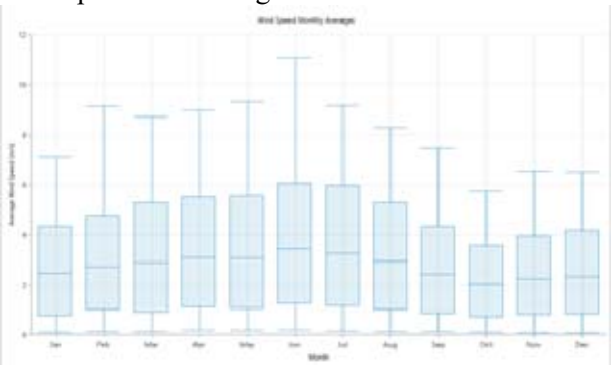

Figure 10: Average daily wind speeds for each month at Sandwip

Figure 11: Monthly wind distribution at Sandwip

An estimate of the residential load was modeled and loaded into HOMER. A typical daily load profile is shown in Figure 12 and can be seen to increase around 6 AM and maintain stability throughout the day until peaking at 6 pm. The results are summarized in Table 2. The average daily energy consumption is 10.6 *kWh/day* and the average power is 0.442 *kW* with a maximum power consumption of 2.5 *kW*. The load factor of the residential load is 0.177 showing that the load is highly variable.

Figure 12: Typical daily profile (Residential Load)

Table 2: Summary of residential load

Residential Load	
Average (kWh/d)	10.6
Average (kW)	0.44
Peak(kW)	2.5
Load factor	0.177

An estimate of the Commercial load is shown in Figure 13. A summary of the commercial load profile is presented in table 3. The commercial load starts to increase around 7 am and is then constant until 6 pm when the load starts to decrease until the idle rate of power consumption.

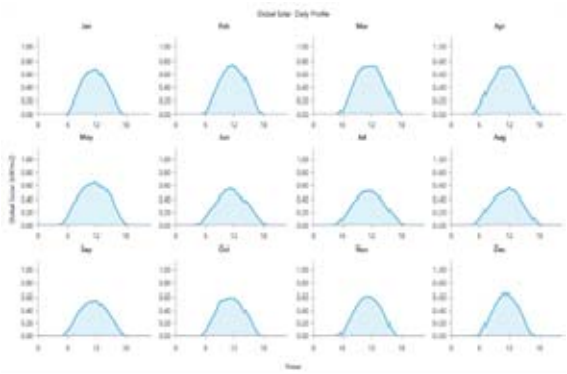

Figure 13: Typical daily profile (Commercial Load)

Table 3: Summary of commercial load

Commercial Load	
Average (kWh/d)	1975
Average (kW)	82
Peak (kW)	400
Load factor	0.205

A financial analysis was conducted using HOMER, which uses the calculation and comparison method to optimize the capacities of components [7]. The most cost-effective solution that was able to satisfy the load requirements was calculated for the three following scenarios:

- An alternating current microgrid with diesel only generation.
- An alternating microgrid with renewable energy generation, batteries and a converter.
- A direct current microgrid with renewable energy generation and batteries.

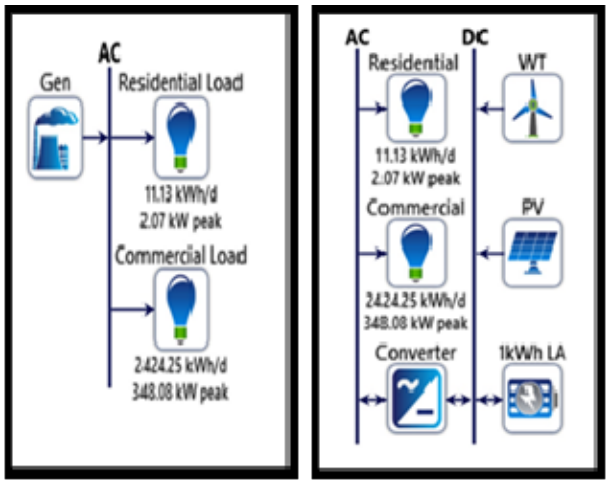

(a) AC Diesel Microgrid (b) AC-DC Hybrid Microgrid

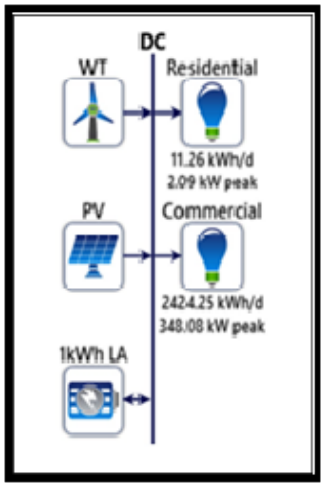

(c) DC Hybrid Microgrid

Figure 14: Microgrid Options

The microgrids were ranked by net present cost (NPC) and the system with the lowest levelized cost of electricity (LCOE) was chosen.

Table 4 lists the sizing of the components for the most cost effective microgrid for each scenario from 35,502 simulations with the one-line diagrams shown in Figure 14. A hybrid microgrid combines two or more sources of renewable energy generation [12]. Note that both hybrid microgrids contain mostly solar generation. This is because the wind resource in Sandwip is relatively low and the solar resource is strong. Also, the price of solar panels is very cheap compared to the same amount of power from wind turbines. These turbines may help to provide energy at night when the solar panels are

redundant and add to the energy diversity of the system.

Table 4: Microgrid optimized sizing

AC Diesel Microgrid

Component	Name	Size	Unit
Generator	Autosize Genset	390	kW
Dispatch Strategy	Homer Cycle Charging		

AC-DC Hybrid Microgrid
DC Hybrid Microgrid

Component	Name	Size	Unit
PV	Generic flat plate PV	1,142	kW
Storage	Generic 1 kWh lead Acid	3,656	Strings
Wind Turbine	Generic 3 kW	2	ea.
Dispatch Strategy	Homer Cycle Charging		

A financial analysis was conducted using HOMER to find the most economical microgrid in terms of NPC. HOMER models the system components, energy resources and loads on an hourly basis [4]. The financial results for each microgrid are listed in Table 5. The AC diesel microgrid has the lowest initial capital costs but because of the high price of diesel fuel, the systems overall NPC is the highest at 78.19cr Tk resulting in an LCOE of 60.02Tk/kWh. The AC-DC hybrid microgrid is an improvement from the diesel-only system but has the highest initial capital costs because more renewable generation and converters are needed to be purchased. The AC-DC hybrid microgrid results in an overall NPC of 55.08cr Tk and an LCOE of 49.98Tk/kWh. The DC hybrid microgrid has the lowest overall NPC. This is because the efficiency of the microgrid is increased due to there being no conversion losses. This means that the load requirements can be met with less PV generation decreasing the capital costs. The decreased sizing of the microgrid, in turn, reduces the replacement and O&M costs. The DC hybrid microgrid has a total cost of 40.5cr Tk resulting in an LCOE of 36.89Tk/kWh. The DC hybrid microgrid is 14.51cr Tk cheaper than the AC hybrid microgrid. Furthermore, the DC hybrid microgrid was shown to be more cost-effective by only modelling the inverter losses on the generation side. In reality, DC circuits have been shown to provide energy savings in solar PV microgrids with battery storage by 14-25% [2]. Therefore, the DC system would have a reduced load profile providing extra cost savings on generation.

Component	Name	Size	Unit
PV	Generic flat plate PV	1,124	kW
Storage	Generic 1 kWh lead Acid	4,482	Strings
Wind Turbine	Generic 3 kW	5	ea.
System Converter	System Converter	306	kW
Dispatch Strategy	Homer Cycle Charging		

Table 5: Summary of microgrid net present cost

Microgrid	AC Diesel	AC-DC Hybrid	DC Hybrid
Capital (Tk)	19.9cr	30.04cr	28.34cr
Operating (Tk)	11.03cr	17.73cr	5.86cr
Replacement (Tk)	16.54cr	12.13cr	11.03cr
Salvage (Tk)	-0.25cr	-4.89cr	-4.73cr
Resource (Tk)	30.97cr	0.00	0.00
Total (Tk)	78.19cr	55.01cr	40.5cr
LCOE(Tk/kWh)	69.02	49.98	36.89

Table 6 shows the current financial scenario of electricity generation of whole Sandwip which is collected physically from Sandwip. The authority supplies electricity to some parts of Sandwip from 6 pm to 12 am through a generator that covers around 2000 people to use electricity [13]. As we can see, the capital and operating cost is comparatively very high compared to DC hybrid microgrid, which is our proposed design.

Table 6: Current scenario of Sandwip (Practical data)

Component	Capital (Tk)	Operating (Tk)	Total (Tk)
Generator	91.1cr	10.1cr	101.2cr

The DC microgrid was constructed in Simulink as shown in Figure 15. The DC microgrid consists of solar generation, wind generation, a commercial load, and a residential load. The power flow is controlled by a charge controller which controls the flow of power between the microgrid and the battery by activating the bidirectional converter. The scopes were set up to view the flow of power in the microgrid and monitor relevant parameters. The power from the renewable energy sources was received from HOMER and entered into Simulink via lookup tables. The Simulink data then drives a current controlled source to turn the values into the current for use within Simulink. The load data was also entered into Simulink via lookup tables.

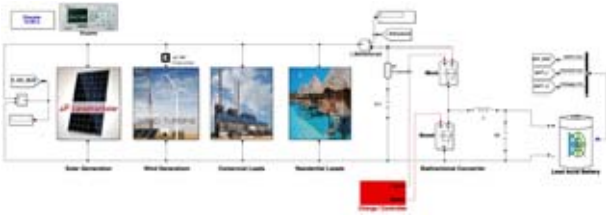

Figure 15: The DC Microgrid in Simulink.

V. Conclusions

The following conclusions can be made from this paper:

1. Presently in Sandwip Island, the authority supply electricity to some parts through a diesel-based generator which covers a small portion from the total consumers. If the total consumers of Sandwip to be covered with diesel-based generator then there will be required huge capital and it is way more costly compared to our proposed microgrid design for Sandwip. Therefore, a DC microgrid is designed based on renewable energy which will be more feasible than the diesel-based generator electricity generation.

2. Power electronic converters can be used in conjunction with solar modules and maximum power point trackers to increase the extracted energy from the solar resource by achieving impedance matching between the source and load.

3. A bidirectional converter can be used in between a microgrid and battery in for power transfer to occur between the microgrid and battery. A PI controller can adequately control the operation of the bidirectional converter to achieve a stable DC bus voltage with a low steady-state error.

4. A lead-acid battery can be modeled in Simulink using the Shepherd Model. Lead acid batteries have a lower energy density than lithium-ion batteries but due to their low price, they are frequently used in microgrids. However, due to their lower energy density, they take up more space.

5. The analysis of the wind resource in HOMER suggests that further investment should not be made on wind turbines. The technical analysis showed that more energy can be extracted from solar panels in conjunction with batteries at a cheaper price.

6. A DC hybrid microgrid provides overall cost savings as compared to an AC diesel-only microgrid because the high price of diesel fuel increases the LCOE of a diesel-only system.

7. A DC hybrid microgrid requires a lower initial capital investment as compared to an AC-DC hybrid microgrid due to the absence of losses in the inverters. This enables the DC microgrid to meet the load requirements with less generation which also reduces the replacement and O&M costs.

8. Designing a microgrid based on 100% renewable energy can create a large system to meet the load on days when renewable energy generation is low. This creates an excess amount of energy generation throughout the year. A trade-off could be to

design the system so that the renewable component meets the baseload and diesel generators are activated to meet the peak load. A larger battery could be used but this would increase the LCOE of the system.

9. Space restrictions and disposal issues can occur when using batteries for storage in a microgrid. If renewable energy generation is low in the region of weeks, the size of the battery required for autonomy would be significantly large.

References

(1) A. T. Elsayed, A. A. Mohamed, and O. A. Mohammed, *"DC microgrids and distribution systems: An overview*", Electric Power Systems Research, vol. 119, pp. 407–417, 2015.

(2) B. Glasgo, I. L. Azevedo, and C. Hendrickson, "How much electricity can we save by using direct current circuits in homes? Understanding the potential for electricity savings and assessing feasibility of a transition towards DC powered buildings", Applied Energy, vol. 180, pp. 66–75, 2016.

(3) C. Li, *"Development of Simscape simulation model for power system stability analysis",* in Power and Energy Engineering Conference (APPEC), 2012 Asia-Pacific, IEEE, 2012, pp.1–4.

(4) H. Energy, "Getting Started Guide for HOMER (Pro Edition-Version 3.13.3)", HOMER Energy: Boulder, Colorado, 2011.

(5) H. Energy, "Getting Started Guide for HOMER Legacy (Version 3.13.3)", HOMER Energy: Boulder, Colorado, 2019

(6) J. B. Ekanayake, N. Jenkins, K. Liyanage, J. Wu, and A. Yokoyama, Smart grid: technology and applications. John Wiley & Sons, 2012

(7) J. Xiao, L. Bai, F. Li, H. Liang, and C. Wang, *"Sizing of energy storage and diesel generators in an isolated microgrid using discrete Fourier transform (DFT)*", IEEE Transactions on Sustainable Energy, vol. 5, no. 3,pp. 907–916, 2014

(8) J. V. R. V. Madhavi, "Modelling and Coordination Control of Hybrid AC/DC Microgrid", International Journal of Emerging Technology and Advanced Engineering, 2014.

(9) M. Starke, L. M. Tolbert, and B. Ozpineci, *"AC vs. DC distribution: A loss comparison*", in Transmission and Distribution Conference and Exposition, 2008. T&D. IEEE/PES, IEEE, 2008, pp. 1–7

(10) R. W. Wies, R. A. Johnson, A. N. Agrawal, and T. J. Chubb, "*Simulink model for economic analysis and environmental impacts of a PV with diesel-battery system for remote villages*", IEEE Transactions on Power Systems, vol. 20, no. 2, pp. 692–700, 2005.

(11) S. Sumathi, L. A. Kumar, and P. Surekha, "*Solar PV and Wind Energy Conversion Systems: An Introduction to Theory, Modeling with MATLAB/SIMULINK*", and the Role of Soft Computing Techniques. Springer, 2015

(12) S. Bensmail, D. Rekioua, and H. Azzi, "*Study of hybrid photovoltaic/fuel cell system for stand-alone applications*", International Journal of Hydrogen Energy, vol. 40, no. 39, pp. 13 820–13 826, 2015

(13) www.energybangla.com/sandwip. (27-10-2019)